COMPUTATIONAL MATHEMATICS
ВЫЧИСЛИТЕЛЬНАЯ МАТЕМАТИКА

UDC 519.6

Original Empirical Research

https://doi.org/10.23947/2587-8999-2025-9-3-30-43

Modelling Circulation in Blood Vessel Aneurysms

Natalya K. Volosova[1], Konstantin A. Volosov[2], Aleksandra K. Volosova[2], Mikhail I. Karlov[3], Dmitriy F. Pastukhov[4] ✉, Yuriy F. Pastukhov[4]

[1] MGTU named after. N.E. Bauman, Moscow, Russian Federation

[2] Russian University of Transport, Moscow, Russian Federation

[3] Moscow Institute of Physics and Technology (National Research University), Dolgoprudny, Russian Federation

[4] Polotsk State University named after Euphrosyne of Polotsk, Novopolotsk, Republic of Belarus

✉ dmitrij.pastuhov@mail.ru

Abstract

Introduction. A two-dimensional hydrodynamic problem in the "stream function–vorticity" variables is numerically solved in an open rectangular cavity simulating blood flow in a blood vessel aneurysm. Two solution algorithms are proposed for Reynolds numbers Re < 1 and for Re ≥ 1.

Materials and Methods. To accelerate the numerical solution with an explicit finite-difference scheme for the vorticity dynamics equation, the initial condition damping method, the n-fold splitting method of the explicit finite-difference scheme (n = 100, 200), and the symmetry plane of the rectangular cavity–aneurysm were employed. In the splitting method, the maximum time step proportional to the square of the spatial step was used without violating the spectral stability of the explicit scheme in the vorticity equation. On half of the rectangular aneurysm, symmetric solutions were considered with a uniform 100 × 50 grid and equal steps $h_1 = h_2 = 0.01$. The inverse matrix for solving the Poisson equation in the "stream function–vorticity" variables with a finite number of elementary operations was computed using the MSIMSL library.

Results. The numerical solution showed that the number and location of circulation regions in the aneurysm at small Reynolds numbers depend on the ratio of the vessel diameter to the aneurysm diameter. At small values of this parameter, the aneurysm contains a single large vortex that narrows the vessel lumen in the case of thrombus formation inside the aneurysm. The narrowing of the blood flow tube inside the aneurysm reaches 34%. It was found that the formation of the hydrodynamic structure in the aneurysm occurs in a time negligible (0.002%) compared to the period between pulsation waves (1 s). For the first time, a boundary condition with fourth-order accuracy was proposed to relate velocity, vorticity, and stream function.

Discussion and Conclusion. The approximation of the equations in systems (4) and (22) has sixth-order accuracy at interior nodes and fourth-order accuracy at boundary nodes. The problem was also solved for blood motion in arteries at high Reynolds numbers (Re = 1500). The solution shows that in the aneurysm symmetry plane a chain of connected vortices is formed with alternating signs of vorticity, carried by the blood flow along the vessel. The initial–boundary value problems (4), (22) formulated in this work make it possible to qualitatively model blood flow in aneurysms of capillaries, arterioles, and arteries at low and high velocities, as well as blood motion in elements of medical equipment.

Keywords: hydrodynamics, numerical methods, partial differential equations, initial–boundary value problem, aneurysm

For Citation. Volosova N.K., Volosov K.A., Volosova A.K., Karlov M.I., Pastukhov D.F., Pastukhov Yu.F. Modelling Circulation in Blood Vessel Aneurysms. *Computation Mathematics and Information Technologies*. 2025;9(3):30–43. https://doi.org/10.23947/2587-8999-2025-9-3-30-43

Оригинальное эмпирическое исследование

Моделирование циркуляции в аневризмах кровеносных сосудов

Н.К. Волосова[1], К.А. Волосов[2], А.К. Волосова[2], М.И. Карлов[3], Д.Ф. Пастухов[4]✉, Ю.Ф. Пастухов[4]

[1] Московский государственный технический университет им. Н.Э. Баумана, г. Москва, Российская Федерация

[2] Российский университет транспорта, г. Москва, Российская Федерация

[3] Московский физико-технический институт (национальный исследовательский университет), г. Долгопрудный, Российская Федерация

[4] Полоцкий государственный университет им. Евфросинии Полоцкой, г. Новополоцк, Республика Беларусь

✉ dmitrij.pastuhov@mail.ru

Аннотация

Введение. Численно решается двумерная гидродинамическая задача в переменных «функция тока — вихрь» в открытой прямоугольной каверне, моделирующей течение крови в аневризме кровеносного сосуда. Предложены два алгоритма решения задачи для чисел Рейнольдса $Re < 1$ и для чисел $Re \geq 1$.

Материалы и методы. Для ускорения численного решения задачи с явной разностной схемой уравнения динамики вихря использовался метод торможения начальных условий, метод n-кратного расщепления явной разностной схемы ($n = 100, 200$) и наличие плоскости симметрии прямоугольной области каверны — аневризмы. В методе расщепления используется максимальный шаг времени, пропорциональный квадрату координатного шага без нарушения спектральной устойчивости явной схемы в уравнении вихря. На половине прямоугольной аневризмы рассматривались симметричные решения и применялась равномерная сетка 100 × 50 с равным шагом $h_1 = h_2 = 0{,}01$. Обратная матрица для решения уравнения Пуассона в переменных «функция тока — вихрь» за конечное число элементарных операций вычислялась библиотекой Msimsl.

Результаты исследования. Численное решение задачи показало, что число и расположение областей циркуляции крови в аневризме при небольших числах Рейнольдса зависят от параметра отношения диаметра сосуда к диаметру аневризмы. Именно при небольшом значении этого параметра аневризму занимает один большой вихрь и сужает просвет сосуда в случае образования тромба внутри аневризмы. Сужение диаметра трубки тока крови внутри аневризмы достигает 34 %. Обнаружено, что формирование гидродинамической структуры в аневризме происходит за время, малое (0,002 %) по сравнению с периодом между пульсационными волнами (1с). Впервые предложено краевое условие с четвертым порядком погрешности для связи скорости, вихря и функции тока.

Обсуждение. Аппроксимация уравнений в системах (4) и (22) имеет шестой порядок погрешности во внутренних и четвертый в граничных узлах. Задача решена также для движения крови в артериях при больших числах Рейнольдса ($Re = 1500$). Ее решение показывает, что в плоскости симметрии аневризмы образуется цепочка связанных вихрей с чередованием знака функции вихря и сносимых кровью вдоль кровеносного сосуда.

Обсуждение и заключение. Сформулированные в работе начально-краевые задачи (4), (22) позволят качественно моделировать движение крови в аневризмах капилляров, артериол и артерий кровеносных сосудов при малых и больших скоростях, а также движение крови в элементах медицинского оборудования.

Ключевые слова: гидродинамика, численные методы, уравнения в частных производных, начально-краевая задача, аневризма

Для цитирования. Волосова Н.К., Волосов К.А., Волосова А.К., Карлов М.И., Пастухов Д.Ф., Пастухов Ю.Ф. Моделирование циркуляции в аневризмах кровеносных сосудов. *Computational Mathematics and Information Technologies*. 2025;9(3):30–43. https://doi.org/10.23947/2587-8999-2025-9-3-30-43

Introduction. This study models a two-dimensional hydrodynamic problem of blood flow in an open rectangular cavity in the “stream function–vorticity” formulation [1]. The velocity field exhibits four corner singular points at the inlet and outlet segments of the cavity–aneurysm, since the streamlines at these points may undergo a 90-degree deflection. Consequently, steep velocity gradients appear in these regions, and the points act as sources of vortices under high blood flow velocity. The present work employs the initial velocity field damping method described in [2]. References [3–7], [8] are related to the solution of two-dimensional hydrodynamic problems or to their high-accuracy approximation. Study [7] specifically addresses blood flow and coagulation processes in blood vessels. In the present research, the *n*-fold splitting method of the vorticity equation ($n = 100, 200$) with an explicit finite-difference scheme, as introduced in [9], is applied. Due to the symmetry of the rectangular cavity (aneurysm), the computational cost can be reduced by half by solving the problem only on one side of the rectangle.

Materials and Methods

Problem Statement. In the two-dimensional formulation, we consider the flow of fluid (blood) in a rectangular cavity–aneurysm, which defines the geometry of the problem. Therefore, it is convenient to adopt a rectangular coordinate system with a uniform grid $n_1 \times n_2 = 100 \times 100$.

We derive the Poiseuille formula for the velocity profile $u(y)$ of plane fluid flow between two parallel rectangular plates. In Fig. 1, the center of the rectangular coordinate system coincides with the symmetry center of a liquid parallelepiped with side lengths $2y \cdot l \cdot b$, with edge length b perpendicular to the plane of the figure. Pressure values p_1, p_2 act on the left and right faces, respectively; the pressure is constant along the y-axis and varies along the x-axis. The difference in pressure forces is equal to $\Delta F_p = (p_1 - p_2)2yb = \frac{p_1 - p_2}{l} 2ybl = \frac{\Delta p}{\Delta x} 2ybl$. This pressure force difference ΔF_p is balanced by the viscous friction force acting on the lower and upper faces of the block.

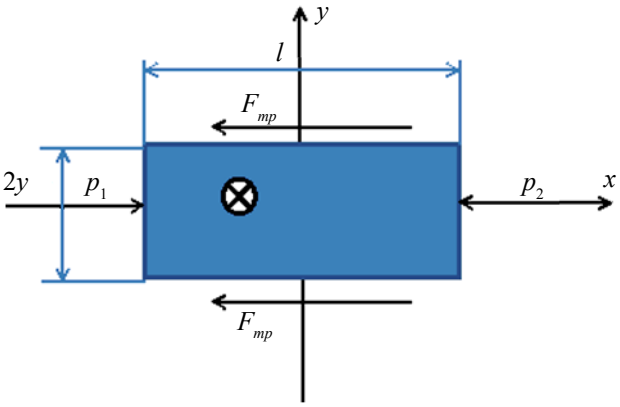

Fig. 1. Illustration of the Poiseuille formula for plane fluid flow

The difference in forces is given by:

$$\Delta F_p = \frac{\Delta p}{\Delta x} 2ybl = 2F_{mp} = 2bl\mu \frac{du}{dy} \Leftrightarrow \frac{du}{dy} = \frac{1}{\mu} \frac{\Delta p}{\Delta x} y \Leftrightarrow u(y) = C_1 y^2 + C_2, C_1 = \frac{1}{2\mu} \frac{\Delta p}{\Delta x} = const.$$

Let us denote the half-width of the plane channel for fluid motion as the velocity of the fluid on the symmetry plane as $u_{\max}$ and determine the unknown constants C_1, C_2 from the no-slip condition on the rigid rectangular plates:

$$u(\Delta) = 0 \Leftrightarrow C_1 \Delta^2 + C_2 = 0, u(0) = C_2 = u_{\max}, C_1 = -\frac{C_2}{\Delta^2} = -\frac{u_{\max}}{\Delta^2}, u(y) = u_{\max}\left(1 - \frac{y^2}{\Delta^2}\right). \quad (1)$$

An aneurysm represents a small segment of a blood vessel whose diameter usually exceeds the vessel diameter by a factor of about two. The aneurysm length L is typically comparable to its diameter $2H$, where H is the aneurysm half-width. To simplify the problem in the rectangular coordinate system, we assume that in an infinite rectangular region between the upper and lower plates a plane fluid flow is formed with the velocity profile (1). A rectangular cavity with inlet and outlet will be referred to as an *open cavity*.

For further simplification, we also assume that the velocity profile (1) is preserved at the inlet to the rectangular aneurysm and at the outlet from it within a narrow symmetric strip relative to the plane $0xz$ of width $2\Delta = 2d$. To accelerate the numerical solution, we exploit symmetry by considering only half of the aneurysm and two halves of the rectangular channel supplying and removing the fluid. According to the symmetry principle, we seek solutions in which, on the symmetry axis, the velocity of fluid particles is directed along the axis at every point; its magnitude may vary numerically, but its direction remains unchanged.

In Fig. 2, the origin of the coordinate system coincides with the lower-left corner of the aneurysm; the x-axis is directed to the right, and the y-axis is directed upward. Let denote $(u(x,y),v(x,y))$ the velocity vector of a fluid particle. On the rigid boundary-namely, on the lower segment and on the lower portions of the side segments of height $H–d$ of the rectangular cavity — the velocity is zero (no-slip condition). Therefore, the stream function on this boundary can be taken as zero. In addition, the normal velocity component is zero on the upper segment of the rectangular cavity $v(x,H) = 0, 0 \le x \le L$.

It is necessary to modify the boundary conditions for velocity and stream function in the formulation of the classical hydrodynamic problem in the "stream function–vorticity" variables for a rectangular cavity, as considered in [1, 2].

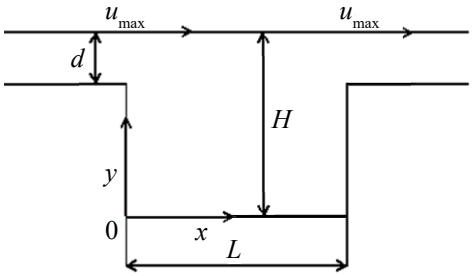

Fig. 2. Geometry of the computational domain

We rewrite the velocity profile (1), taking into account the shift of the coordinate origin shown in Fig. 2:

$$y = \bar{y} + H, u(\bar{y}) = u(y - H) = u_{\max}\left(1 - \frac{(y-H)^2}{\Delta^2}\right), y \in [H - \Delta, H]. \tag{2}$$

Integrating equation (2) with respect to y, and taking into account the relation $u = \psi_y$, we obtain the dependence of the stream function in the gaps along the side walls of the cavity:

$$\begin{gathered}\psi(y) = u_{\max}\left(y - \frac{(y-H)^3}{3\Delta^2}\right) + C_0, \psi(H-\Delta) = 0 \Leftrightarrow C_0 = -u_{\max}\left(H - \frac{2}{3}\Delta\right), \\ \psi(0,y) = \psi(L,y) = \begin{cases} 0, y \in [0, H-\Delta], \\ u_{\max}\left(y + \frac{2}{3}\Delta - H - \frac{(y-H)^3}{3\Delta^2}\right), y \in [H-\Delta, H]. \end{cases}\end{gathered} \tag{3}$$

As in [2], we denote the characteristic length by L, time by $\frac{L}{u_{\max}}$, velocity by $u_{\max}$, stream function by $Lu_{\max}$, vorticity by $\frac{u_{\max}}{L}$, and Reynolds number by Re. We introduce the following dimensionless variables: the horizontal coordinate is denoted by $\bar{x}$, the vertical coordinate by $\bar{y}$, the stream function and vorticity by $\bar{\psi}, \bar{w}$, respectively, the velocity vector by $(\bar{u}, \bar{v})$, and time by $\bar{t}$. These quantities are nondimensionalized as follows:

$$0 \le \bar{x} = \frac{x}{L} \le 1,\ 0 \le \bar{y} = \frac{y}{L} \le k = \frac{H}{L}, \bar{\psi} = \frac{\psi}{\psi_{\max}}, \psi_{\max} = Lu_{\max},$$

$$\bar{u} = \frac{u}{u_{\max}}, \bar{v} = \frac{v}{u_{\max}} \bar{w} = \frac{w}{w_{\max}}, w_{\max} = \frac{u_{\max}}{L},$$

$$\bar{t} = \frac{t}{T}, T = \frac{L}{u_{\max}}, \mathrm{Re} = \frac{u_{\max} L}{\nu}.$$

The kinematic viscosity of blood is $\nu = \frac{\mu}{\rho} = \frac{3{,}5 \cdot 10^{-3}\, Па \cdot с}{1050\, кг/м^3} = 3{,}33(3) \cdot 10^{-6} \frac{м^2}{с}$.

The hydrodynamic system in nondimensional variables and functions, following [1, 2], for an open cavity at high Reynolds numbers can be written as:

$$\begin{cases} \bar{\psi}_{\bar{x}\bar{x}} + \bar{\psi}_{\bar{y}\bar{y}} = -\bar{w}(\bar{x}, \bar{y}),\ 0 < \bar{x} = \frac{x}{L} < 1,\ 0 < \bar{y} < k_{\max}, \\ \bar{w} = \bar{v}_{\bar{x}} - \bar{u}_{\bar{y}}, \\ \bar{u} = \bar{\psi}_{\bar{y}}; \bar{v} = -\bar{\psi}_{\bar{x}}, \\ \bar{w}_{\bar{t}} + \bar{u} \cdot \bar{w}_{\bar{x}} + \bar{v} \cdot \bar{w}_{\bar{y}} = \frac{1}{\mathrm{Re}}\left(\bar{w}_{\bar{x}\bar{x}} + \bar{w}_{\bar{y}\bar{y}}\right), 0 < \bar{t} = \frac{t}{T}, \\ \bar{\psi}\big|_{\Gamma 1} \equiv 0, \bar{v}\big|_{\Gamma} \equiv 0, \bar{u}\big|_{\Gamma_1} = 0, \bar{v}\big|_{\Gamma_2} = 0, \\ \psi(0,y) = \psi(L,y) = \begin{cases} 0, y \in [0, H-\Delta], \\ u_{\max} L\left(\frac{y}{L} + \frac{2}{3}\frac{\Delta}{L} - \frac{H}{L} - \frac{(y/L - H/L)^3}{3(\Delta/L)^2}\right), y \in [H-\Delta, H], \\ \frac{2}{3} u_{\max} \Delta, y = H, \end{cases} \end{cases} \tag{4}$$

$$\overline{u}(0,y)=\overline{u}(L,y)=\frac{u(y)}{u_{\max}}=\begin{cases}0, y\in[0,H-\Delta],\\ \left(1-\dfrac{(y-H)^2}{\Delta^2}\right), y\in[H-\Delta,H],\end{cases}$$

$$\overline{\psi}(0,\overline{y})=\overline{\psi}(L,\overline{y})=\frac{\psi(0,y)}{\psi_{\max}}=\begin{cases}0, y\in[0,H-\Delta],\\ \left(\overline{y}+\dfrac{2}{3}\Delta/L-H/L-\dfrac{(\overline{y}-H/L)^3}{3(\Delta/L)^2}\right), \overline{y}\in[(H-\Delta)/L,H/L],\\ \dfrac{2}{3}\dfrac{\Delta}{L}, \overline{y}=H/L.\end{cases}$$

Here Γ_1 denotes the union of the lower side segments and the bottom boundary, Γ_2 corresponds to the upper segment of the rectangle Γ. The first equation in system (1) is the Poisson equation for the stream function and vorticity. The two-dimensional Poisson equation on the rectangle is solved in matrix form with a finite number of arithmetic operations and sixth-order accuracy [2]. Below, for brevity, we omit the overbars on nondimensional functions, time, and coordinates, except in formulas (24).

The second line of system (4) defines vorticity in terms of the velocity field derivatives. The third line gives the velocity components as derivatives of the stream function. The fourth equation is the vorticity dynamics equation, which is the only time-dependent equation in system (1). On the left-hand side, it contains the full (convective) time derivative.

On the boundary of the rectangle, the vertical velocity component is zero; the horizontal component is unspecified on the upper boundary, set to zero on the lower boundary, and described by formula (1) on the side boundaries.

Using the method of undetermined coefficients [10], the velocity on the upper boundary is specified by the quadrature formula (5.1) with tenth-order accuracy in problems (4) (Re = 1500) and (22) (Re = 0.75). Formula (5.1) is applied only to problem (4).

$$u(n_2,j)=\psi_y(n_2,j)=\frac{1}{(-h_2)}\left(-\frac{83711}{27720}\psi_{n_2,j}+11\psi_{n_2-1,j}-\frac{55}{2}\psi_{n_2-2,j}+55\psi_{n_2-3,j}-\frac{165}{2}\psi_{n_2-4,j}+\frac{462}{5}\psi_{n_2-5,j}-\right.$$
$$\left.-77\psi_{n_2-6,j}+\frac{330}{7}\psi_{n_2-7,j}-\frac{165}{8}\psi_{n_2-8,j}+\frac{55}{9}\psi_{n_2-9,j}-\frac{11}{10}\psi_{n_2-10,j}+\frac{1}{11}\psi_{n_2-11,j}\right)+O\left(h^{10}\right), j=\overline{1,n_1-1}, \quad (5.1)$$

$$u(n_2,j)=\frac{1}{(-h_2)}\left(-\frac{137}{60}\psi_{n_2,j}+5\psi_{n_2-1,j}-5\psi_{n_2-2,j}+\frac{10}{3}\psi_{n_2-3,j}-\frac{5}{4}\psi_{n_2-4,j}+\frac{1}{5}\psi_{n_2-5,j}\right)+O\left(h^4\right), j=\overline{1,n_1-1}. \quad (5.2)$$

Following [2], we choose a nonzero and continuous initial velocity field in the central part of the cavity:

$$\overline{u}(x_m y_n)=\begin{cases}0, y_m\in[0,H-\Delta],\\ \left(1-\dfrac{(y_m-H)^2}{\Delta^2}\right), y_m\in[H-\Delta,H], y_m=mh_2, m=\overline{0,n_2}, x_n=nh_1, n=\overline{0,n_1}\end{cases}$$
$$\overline{v}(x_m y_n)=0, y_m=mh_2, m=\overline{0,n_2}, x_n=nh_1, n=\overline{0,n_1}. \quad (6)$$

In the new hydrodynamic problem for an open rectangular cavity in the "stream function–vorticity" variables, where the velocity on the upper segment of the cavity is evaluated by formulas (5), we specify the computational sequence, since it differs substantially from the algorithm described in [1]:

1 step: impose the (time-invariant) boundary conditions on the rectangle boundary for the stream function and for the vertical component of velocity;

2 step: modify the right-hand side of the Poisson equation for the stream function (i.e., the vorticity term) according to formulas (12), (13);

3 step: solve the Poisson equation ((7)–(11)), i.e. find the stream-function values at the interior grid points of the rectangular mesh;

4 step: compute the velocity on the upper segment of the cavity using formulas (5);

5 step: compute the new velocity field at interior grid nodes (formula (18));

6 step: obtain new boundary values of vorticity using formulas (24);

7 step: compute new vorticity values at interior nodes via equation (19).

After step 7 the cycle returns to step 1.

We now describe each step in greater detail. According to [1], the first equation of system (1) — the Poisson equation — is solved by a matrix method in a finite number of elementary operations [2] with sixth-order accuracy at interior points:

$$\Delta\psi = \psi_{xx} + \psi_{yy} = f(x,y) = -w \Leftrightarrow \frac{1}{h^2}\left(-\frac{10}{3}\psi_{0,0} + \frac{2}{3}\left(\psi_{-1,0} + \psi_{0,-1} + \psi_{1,0} + \psi_{0,1}\right) + \frac{1}{6}\left(\psi_{-1,-1} + \psi_{1,-1} + \psi_{-1,1} + \psi_{1,1}\right)\right) =$$
$$= f + \frac{h^2}{12}\left(f_{xx} + f_{yy}\right) + \frac{h^4}{360}\left(f_x^{(4)} + f_y^{(4)}\right) + \frac{h^4 f_{xxyy}^{(4)}}{90} + O\left(h^6\right). \quad (7)$$

To solve Poisson equation (7) for the stream function in system (4) with accuracy $O(h^6)$ we set $f = -w$, represent the derivatives f_{xx}, f_{yy} with accuracy $O(h^4)$, and approximate $f_x^{(4)}, f_y^{(4)}, f_{xxyy}^{(4)}$ with accuracy $O(h^2)$.

In [2, 10], by the method of undetermined coefficients, formulas for the interior-node values of a function f with indices $n = \overline{2, n_1 - 2}, m = \overline{2, n_2 - 2}$ were obtained:

$$\begin{cases} f_{xx} + f_{yy} = \frac{1}{h^2}\left(-5f_{0,0} + \frac{4}{3}\left(f_{-1,0} + f_{0,-1} + f_{1,0} + f_{0,1}\right) - \frac{1}{12}\left(f_{-2,0} + f_{0,-2} + f_{2,0} + f_{0,2}\right)\right) + O\left(h^4\right), \\ f_x^{(4)} + f_y^{(4)} = \frac{1}{h^4}\left(12f_{0,0} - 4\left(f_{-1,0} + f_{0,-1} + f_{1,0} + f_{0,1}\right) + f_{-2,0} + f_{0,-2} + f_{2,0} + f_{0,2}\right) + O\left(h^2\right), \\ f_{xxyy}^{(4)} = \frac{1}{h^4}\left(4f_{0,0} - 2\left(f_{-1,0} + f_{0,-1} + f_{1,0} + f_{0,1}\right) + f_{-1,-1} + f_{-1,1} + f_{1,-1} + f_{1,1}\right) + O\left(h^2\right). \end{cases} \quad (8)$$

Thus, formulas (7) and (8) together approximate the Poisson equation in problems (4) and (22) with accuracy $O(h^6)$ at interior nodes.

Reference [2] describes a matrix method for solving the finite-difference Poisson equation (7) in a finite number of arithmetic operations using a vectorized sweep (block tridiagonal/vector Thomas) method. The finite-difference equation can be written as:

$$\frac{1}{h^2}\left(\frac{-10}{3}\psi_{m,n} + \frac{2}{3}\left(\psi_{m-1,n} + \psi_{m+1,n} + \psi_{m,n-1} + \psi_{m,n+1}\right) + \frac{1}{6}\left(\psi_{m-1,n-1} + \psi_{m+1,n-1} + \psi_{m-1,n+1} + \psi_{m+1,n+1}\right)\right) = f_{m,n} + \frac{h^2}{12}\left(f_{xx} + f_{yy}\right) +$$
$$+h^4\left(\frac{1}{360}\left(f_x^{(4)} + f_y^{(4)}\right) + \frac{1}{90}f_{xxyy}^{(4)}\right) + O\left(h^6\right) \equiv F_{m,n},\ n = \overline{1, n_1 - 1}, m = \overline{1, n_2 - 1}. \quad (9)$$

Define the square matrices A, B of size $(n_1 - 1) \times (n_1 - 1)$:

$$a_{m,n} = \begin{cases} -\frac{10}{3}, m = n; m = \overline{1, n_1 - 1}, n = \overline{1, n_1 - 1}, \\ \frac{2}{3}, m = n + 1 \text{ или } m = n - 1, \\ 0, m \geq n + 2 \text{ или } m \leq n - 2, \end{cases} \qquad b_{m,n} = \begin{cases} \frac{2}{3}, m = n; m = \overline{1, n_1 - 1}, n = \overline{1, n_1 - 1}, \\ \frac{1}{6}, m = n + 1 \text{ или } m = n - 1, \\ 0, m \geq n + 2 \text{ или } m \leq n - 2. \end{cases} \quad (10)$$

In the present work, the matrix algorithm for solving (9) is identical to that in [2]:

1. Using the formula

$$F^T{}_{m,n} = f_{m,n}h^2 + \frac{h^4}{12}\left(f_{xx} + f_{yy}\right) + h^6\left(\frac{1}{360}\left(f_x^{(4)} + f_y^{(4)}\right) + \frac{1}{90}f_{xxyy}^{(4)}\right) + O\left(h^8\right)\Big|_{x = x_n, y = y_m}$$

compute the right-hand side of the Poisson equation at all interior nodes of the uniform rectangular grid (m=1, …, n_2–1; n=1, …, n_1–1).

2. Modify the right-hand sides of the linear system (11) according to formulas (12), (13) at the nodes of the rectangular contour adjacent to the boundary contour, i. e. determine $\overline{F_{m,n}}$ from the values $F_{m,n}$ computed in step 1:

$$\begin{cases} A\psi_1^T + B\psi_2^T = \overline{F_1^T}, \\ B\psi_{m-1}^T + A\psi_m^T + B\psi_{m+1}^T = \overline{F_m^T}, m = \overline{2, n_2 - 2}, \\ B\psi_{n_2-2}^T + A\psi_{n_2-1}^T = \overline{F_{n_2-1}^T}. \end{cases} \quad (11)$$

$$\begin{cases}
\frac{-10}{3}\psi_{1,n_1-1}+\frac{2}{3}\left(\psi_{2,n_1-1}+\psi_{1,n_1-2}+\psi_{1,n_1}+\psi_{0,n_1-1}\right)+\frac{1}{6}\left(\psi_{2,n_1-2}+\psi_{0,n_1-2}+\psi_{2,n_1}+\psi_{0,n_1}\right)=F_{1,n_1-1},\\
\overline{F_{1,n_1-1}}\equiv F_{1,n_1-1}-\frac{2}{3}\left(\psi_{1,n_1}+\psi_{0,n_1-1}\right)-\frac{1}{6}\left(\psi_{0,n_1-2}+\psi_{2,n_1}+\psi_{0,n_1}\right),\\
\frac{-10}{3}\psi_{n_2-1,1}+\frac{2}{3}\left(\psi_{n_2-2,1}+\psi_{n_2-1,2}+\psi_{n_2-1,0}+\psi_{n_2,1}\right)+\frac{1}{6}\left(\psi_{n_2-2,2}+\psi_{n_2,2}+\psi_{n_2-2,0}+\psi_{n_2,0}\right)=F_{n_2-1,1},\\
\overline{F_{n_2-1,1}}\equiv F_{n_2-1,1}-\frac{2}{3}\left(\psi_{n_2-1,0}+\psi_{n_2,1}\right)-\frac{1}{6}\left(\psi_{n_2,2}+\psi_{n_2-2,0}+\psi_{n_2,0}\right),\\
\frac{-10}{3}\psi_{n_2-1,n_1-1}+\frac{2}{3}\left(\psi_{n_2-2,n_1-1}+\psi_{n_2-1,n_1-2}+\psi_{n_2-1,n_1}+\psi_{n_2,n_1-1}\right)+\frac{1}{6}\left(\psi_{n_2-2,n_1-2}+\psi_{n_2,n_1-2}+\psi_{n_2-2,n_1}+\psi_{n_2,n_1}\right)=F_{n_2-1,n_1-1},\\
\overline{F_{n_2-1,n_1-1}}\equiv F_{n_2-1,n_1-1}-\frac{2}{3}\left(\psi_{n_2-1,n_1}+\psi_{n_2,n_1-1}\right)-\frac{1}{6}\left(\psi_{n_2,n_1-2}+\psi_{n_2-2,n_1}+\psi_{n_2,n_1}\right),\\
\frac{-10}{3}\psi_{1,1}+\frac{2}{3}\left(\psi_{2,1}+\psi_{1,2}+\psi_{1,0}+\psi_{0,1}\right)+\frac{1}{6}\left(\psi_{2,2}+\psi_{0,2}+\psi_{2,0}+\psi_{0,0}\right)=F_{1,1},\\
\overline{F_{1,1}}\equiv F_{1,1}-\frac{2}{3}\left(\psi_{1,0}+\psi_{0,1}\right)-\frac{1}{6}\left(\psi_{0,2}+\psi_{2,0}+\psi_{0,0}\right).
\end{cases}\tag{12}$$

$$\begin{cases}
-\frac{10}{3}\psi_{1,n}+\frac{2}{3}\left(\psi_{1,n-1}+\psi_{2,n}+\psi_{1,n+1}+\psi_{0,n}\right)+\frac{1}{6}\left(\psi_{2,n-1}+\psi_{2,n+1}+\psi_{0,n-1}+\psi_{0,n+1}\right)=F_{1,n},n=\overline{2,n_1-2},\\
\overline{F_{1,n}}=F_{1,n}-\frac{2}{3}\psi_{0,n}-\frac{1}{6}\left(\psi_{0,n-1}+\psi_{0,n+1}\right),n=\overline{2,n_1-2},\\
-\frac{10}{3}\psi_{n_2-1,n}+\frac{2}{3}\left(\psi_{n_2-1,n-1}+\psi_{n_2-2,n}+\psi_{n_2-1,n+1}+\psi_{n_2,n}\right)+\frac{1}{6}\left(\psi_{n_2-2,n-1}+\psi_{n_2-2,n+1}+\psi_{n_2,n-1}+\psi_{n_2,n+1}\right)=F_{n_2-1,n},n=\overline{2,n_1-2},\\
\overline{F_{n_2-1,n}}=F_{n_2-1,n}-\frac{2}{3}\psi_{n_2,n}-\frac{1}{6}\left(\psi_{n_2,n-1}+\psi_{n_2,n+1}\right),n=\overline{2,n_1-2},\\
-\frac{10}{3}\psi_{m,1}+\frac{2}{3}\left(\psi_{m-1,1}+\psi_{m,2}+\psi_{m+1,1}+\psi_{m,0}\right)+\frac{1}{6}\left(\psi_{m-1,2}+\psi_{m+1,2}+\psi_{m-1,0}+\psi_{m+1,0}\right)=F_{m,1},m=\overline{2,n_2-2},\\
\overline{F_{m,1}}=F_{m,1}-\frac{2}{3}\psi_{m,0}-\frac{1}{6}\left(\psi_{m-1,0}+\psi_{m+1,0}\right),m=\overline{2,n_2-2},\\
-\frac{10}{3}\psi_{m,n_1-1}+\frac{2}{3}\left(\psi_{m-1,n_1-1}+\psi_{m,n_1-2}+\psi_{m+1,n_1-1}+\psi_{m,n_1}\right)+\frac{1}{6}\left(\psi_{m-1,n_1-2}+\psi_{m+1,n_1-2}+\psi_{m-1,n_1}+\psi_{m+1,n_1}\right)=F_{m,n_1-1},m=\overline{2,n_2-2},\\
\overline{F_{m,n_1-1}}=F_{m,n_1-1}-\frac{2}{3}\psi_{m,n_1}-\frac{1}{6}\left(\psi_{m-1,n_1}+\psi_{m+1,n_1}\right),m=\overline{2,n_2-2},\\
\overline{F_{m,n}}=F_{m,n},\ \forall m\in\overline{2,n_2-2},n\in\overline{2,n_1-2}.
\end{cases}\tag{13}$$

3. Compute the forward sweep (matrix recurrence) coefficients by formulas (14), (15) $m=\overline{1,n_2-2}$:

$$\lambda_1=-A^{-1}B,\nu_1=A^{-1}\overline{F_1^T},\tag{14}$$

$$\lambda_m=-\left(B\lambda_{m-1}+A\right)^{-1}B,\nu_m=\left(B\lambda_{m-1}+A\right)^{-1}\left(\overline{F_m^T}-B\nu_{m-1}\right),m=\overline{2,n_2-2}.\tag{15}$$

4. Compute the solution row vector $\psi_{n_2-1}^T$ by formula (16):

$$\psi_{n_2-1}^T=\left(B\lambda_{n_2-2}+A\right)^{-1}\left(\overline{F_{n_2-1}^T}-B\nu_{n_2-2}\right).\tag{16}$$

5. Compute the remaining rows of the solution matrix $\psi^T{}_m$ using formulas (17):

$$\psi_m^T=\lambda_m\psi_{m+1}^T+\nu_m,m=\overline{n_2-2,1},\nu_{n_2-1}=\psi_{n_2-1}^T.\tag{17}$$

The matrix sweep algorithm (9)–(17) preserves sixth-order accuracy in accordance with formulas (7) and (8) for the Poisson equation.

The second and third equations of system (4) $\overline{w}=\overline{v}_{\overline{x}}-\overline{u}_{\overline{y}},\overline{u}=\overline{\psi}_{\overline{y}},\overline{v}=-\overline{\psi}_{\overline{x}}$ are linear with respect to the first derivatives. We present quadrature formulas for the first derivative with various stencils. For the equation $\overline{u}=\overline{\psi}_{\overline{y}}$ we have:

$$\begin{cases} u_{(i,j)} = \frac{1}{h}\left(\frac{3}{4}\left(\psi_{i+1,j}-\psi_{i-1,j}\right)-\frac{3}{20}\left(\psi_{i+2,j}-u_{i-2,j}\right)+\frac{1}{60}\left(\psi_{i+3,j}-\psi_{i-3,j}\right)\right)+O\left(h^6\right), i=\overline{3,n_2-3}, j=\overline{1,n_1-1}, \\ u_{(1,j)} = \frac{1}{h}\left(-\frac{\psi_{0,j}}{5}-\frac{13}{12}\psi_{1,j}+2\psi_{2,j}-\psi_{3,j}+\frac{\psi_{4,j}}{3}-\frac{\psi_{5,j}}{20}\right)+O\left(h^4\right), j=\overline{1,n_1-1}, \\ u_{(2,j)} = \frac{1}{12h}\left(8\left(\psi_{3,j}-\psi_{1,j}\right)-\left(\psi_{4,j}-\psi_{0,j}\right)\right)+O\left(h^4\right), j=\overline{1,n_1-1}, \\ u_{(n_2-1,j)} = -\frac{1}{h}\left(-\frac{\psi_{n_2,j}}{5}-\frac{13}{12}\psi_{n_2-1,j}+2\psi_{n_2-2,j}-\psi_{n_2-3,j}+\frac{\psi_{n_2-4,j}}{3}-\frac{\psi_{n_2-5,j}}{20}\right)+O\left(h^4\right), j=\overline{1,n_1-1}, \\ u_{(n_2-2,j)} = -\frac{1}{12h}\left(8\left(\psi_{n_2-3,j}-\psi_{n_2-1,j}\right)-\left(\psi_{n_2-4,j}-\psi_{n_2,j}\right)\right)+O\left(h^4\right), j=\overline{1,n_1-1}. \end{cases} \quad (18)$$

Analogous formulas can be written for the equation $\bar{v}=-\overline{\psi}_{\bar{x}}$. To accelerate the numerical solution, the vorticity equation in (4) was treated using the splitting method [9].

Analytically, the *n*-fold splitting method for the vorticity equation over the time interval τ_0 / n can be written as:

$$\frac{w^{k+((i+1)/n)}-w^{k+(i/n)}}{\tau_0/n}+u^k\cdot w_x^{k+(i/n)}+v^k\cdot w_y^{k+(i/n)}=\frac{1}{\mathrm{Re}}\left(w_{xx}^{k+(i/n)}+w_{yy}^{k+(i/n)}\right), i=\overline{0,n-1}. \quad (19)$$

The recurrence system (19) for the vorticity with a frozen velocity field $\left(u^k(x,y),v^k(x,y)\right), i=\overline{0,n-1}, k=const, k=1,2,...$ consists of *n* intermediate steps $i=\overline{0,n-1}$, the superscript *i* denotes the intermediate time-layer index in equation (19), and subscript *k* denotes the multiplicity index of the time layer in system (19). Velocity and stream-function fields remain fixed in equations (19) at values *k* = *const* while the index *i* changes $i=\overline{0,n-1}$. In this system only the vorticity field $w^{k+(i/n)}, i=\overline{0,n-1}$ is updated. The velocity field changes by a jump in systems (4) or in (22), (19) when the time index of the vorticity increases by one (from *k* to *k*+1) in the recurrence system (19).

The idea of splitting system (19) lies in reducing the accumulation of rounding errors and the computational time required for its solution. The differential operators with respect to coordinates in (19) are approximated at interior nodes with accuracy $O(h^6)$, as are all equations of system (4); the boundary conditions are approximated with accuracy $O(h^4)$, and the time derivative with accuracy $O(\tau)$.

Thus, over the time interval τ_0 / n (associated with the reduction of stability due to the presence of four singular points of the velocity field), solving equation (19) *n* times yields a temporal jump of magnitude τ_0 (which is *n* times larger than sequentially solving the full system of equations (4)).

Equation (19) is linear with respect to the coordinate derivatives $w_x^i, w_y^i, w_{xx}^i, w_{yy}^i$. In [9] it was shown that for spectral stability of the vorticity dynamics equation (19), it is sufficient to choose the ratio of the time step and spatial step in the form of the inequality: $\tau_0 \le \frac{3}{16}h^2\,\mathrm{Re}-(4), \left(\tau_0 \le \frac{3}{16}h^2-(22)\right)$.

For the derivative w_y in (19), we write quadrature formulas (the formulas for w_x are analogous):

$$\begin{cases} w_{y(i,j)} = \frac{1}{h}\left(\frac{3}{4}\left(w_{i+1,j}-w_{i-1,j}\right)-\frac{3}{20}\left(w_{i+2,j}-w_{i-2,j}\right)+\frac{1}{60}\left(w_{i+3,j}-w_{i-3,j}\right)\right)+O\left(h^6\right), i=\overline{3,n_2-3}, j=\overline{1,n_1-1}, \\ w_{y(1,j)} = \frac{1}{h}\left(-\frac{w_{0,j}}{5}-\frac{13}{12}w_{1,j}+2w_{2,j}-w_{3,j}+\frac{w_{4,j}}{3}-\frac{w_{5,j}}{20}\right)+O\left(h^4\right), j=\overline{1,n_1-1}, \\ w_{y(2,j)} = \frac{1}{12h}\left(8\left(w_{3,j}-w_{1,j}\right)-\left(w_{4,j}-w_{0,j}\right)\right)+O\left(h^4\right), j=\overline{1,n_1-1}, \\ w_{y(n_2-1,j)} = -\frac{1}{h}\left(-\frac{w_{n_2,j}}{5}-\frac{13}{12}w_{n_2-1,j}+2w_{n_2-2,j}-w_{n_2-3,j}+\frac{w_{n_2-4,j}}{3}-\frac{w_{n_2-5,j}}{20}\right)+O\left(h^4\right), j=\overline{1,n_1-1}, \\ w_{y(n_2-2,j)} = -\frac{1}{12h}\left(8\left(w_{n_2-3,j}-w_{n_2-1,j}\right)-\left(w_{n_2-4,j}-w_{n_2,j}\right)\right)+O\left(h^4\right), j=\overline{1,n_1-1}. \end{cases} \quad (20)$$

The second derivatives w_{yy} in (19) take the form:

$$\begin{cases} w_{yy(i,j)} = \frac{1}{h^2}\left(-\frac{49}{18}w_{i,j}+\frac{3}{2}\left(w_{i+1,j}+w_{i-1,j}\right)-\frac{3}{20}\left(w_{i+2,j}+w_{i-2,j}\right)+\frac{1}{90}\left(w_{i+3,j}+w_{i-3,j}\right)\right)+O\left(h^6\right), i=\overline{3,n_2-3}, j=\overline{1,n_1-1}, \\ w_{yy(1,j)} = \frac{1}{h^2}\left(\frac{137}{180}w_{0,j}-\frac{49}{60}w_{1,j}-\frac{17}{12}w_{2,j}+\frac{47}{18}w_{3,j}-\frac{19}{12}w_{4,j}+\frac{31}{60}w_{5,j}-\frac{13}{180}w_{6,j}\right)+O\left(h^4\right), j=\overline{1,n_1-1}, \\ w_{yy(2,j)} = \frac{1}{h^2}\left(-\frac{5}{2}w_{2,j}+\frac{4}{3}\left(w_{1,j}+w_{3,j}\right)-\frac{1}{12}\left(w_{0,j}+w_{4,j}\right)\right)+O\left(h^4\right), j=\overline{1,n_1-1}, \\ w_{yy(n_2-1,j)} = \frac{1}{h^2}\left(\frac{137}{180}w_{n_2,j}-\frac{49}{60}w_{n_2-1,j}-\frac{17}{12}w_{n_2-2,j}+\frac{47}{18}w_{n_2-3,j}-\frac{19}{12}w_{n_2-4,j}+\frac{31}{60}w_{n_2-5,j}-\frac{13}{180}w_{n_2-6,j}\right)+O\left(h^4\right), j=\overline{1,n_1-1}, \\ w_{yy(n_2-2,j)} = \frac{1}{h^2}\left(-\frac{5}{2}w_{n_2-2,j}+\frac{4}{3}\left(w_{n_2-1,j}+w_{n_2-3,j}\right)-\frac{1}{12}\left(w_{n_2,j}+w_{n_2-4,j}\right)\right)+O\left(h^4\right), j=\overline{1,n_1-1}. \end{cases} \quad (21)$$

Analogous formulas are written for the derivative w_{xx}. Problem (4) and its algorithm (steps (5)–(21), (23), (24)) apply to blood motion in the aorta and arteries at high velocities and large Reynolds numbers. However, at small Reynolds numbers, using the diffusion time scale [9], we arrive at problem (22):

$$\bar{t} = \frac{t}{T}, T_{dif} = T = \frac{L^2}{\nu}, \mathrm{Re} = \frac{u_{\max} L}{\nu},$$

$$0 \le \bar{x} = \frac{x}{L} \le 1,\ 0 \le \bar{y} = \frac{y}{L} \le k = \frac{H}{L}, \bar{\psi} = \frac{\psi}{\psi_{\max}}, \psi_{\max} = L u_{\max},$$

$$\bar{u} = \frac{u}{u_{\max}}, \bar{v} = \frac{v}{u_{\max}} \bar{w} = \frac{w}{w_{\max}}, w_{\max} = \frac{u_{\max}}{L},$$

$$\frac{\partial w}{\partial t} + u\frac{\partial w}{\partial x} + v\frac{\partial w}{\partial y} = \nu\left(\frac{\partial^2 w}{\partial x^2} + \frac{\partial^2 w}{\partial y^2}\right) \Leftrightarrow \frac{1}{T}\frac{\partial \bar{w}}{\partial \bar{t}} + \frac{u_{\max}}{L}\left(\bar{u}\frac{\partial \bar{w}}{\partial \bar{x}} + \bar{v}\frac{\partial \bar{w}}{\partial \bar{y}}\right) = \frac{\nu}{L^2}\left(\frac{\partial^2 \bar{w}}{\partial \bar{x}^2} + \frac{\partial^2 \bar{w}}{\partial \bar{y}^2}\right) \Leftrightarrow$$

$$\frac{\nu}{L^2}\frac{\partial \bar{w}}{\partial \bar{t}} + \frac{u_{\max}}{L}\left(\bar{u}\frac{\partial \bar{w}}{\partial \bar{x}} + \bar{v}\frac{\partial \bar{w}}{\partial \bar{y}}\right) = \frac{\nu}{L^2}\left(\frac{\partial^2 \bar{w}}{\partial \bar{x}^2} + \frac{\partial^2 \bar{w}}{\partial \bar{y}^2}\right) \Leftrightarrow \frac{\partial \bar{w}}{\partial \bar{t}} + \mathrm{Re}\left(\bar{u}\frac{\partial \bar{w}}{\partial \bar{x}} + \bar{v}\frac{\partial \bar{w}}{\partial \bar{y}}\right) = \frac{\partial^2 \bar{u}}{\partial \bar{x}^2} + \frac{\partial^2 \bar{u}}{\partial \bar{y}^2}.$$

$$\begin{cases} \bar{\psi}_{\bar{x}\bar{x}} + \bar{\psi}_{\bar{y}\bar{y}} = -\bar{w}(\bar{x},\bar{y}),\ 0 < \bar{x} = \frac{x}{L} < 1,\ 0 < \bar{y} < k_{\max}, \\ \bar{w} = \bar{v}_{\bar{x}} - \bar{u}_{\bar{y}}, \\ \bar{u} = \bar{\psi}_{\bar{y}}; \bar{v} = -\bar{\psi}_{\bar{x}}, \\ \bar{w}_{\bar{t}} + \mathrm{Re}\left(\bar{u}\cdot\bar{w}_{\bar{x}} + \bar{v}\cdot\bar{w}_{\bar{y}}\right) = \bar{w}_{\bar{x}\bar{x}} + \bar{w}_{\bar{y}\bar{y}}, 0 < \bar{t} = \frac{t}{T}, \\ \bar{\psi}\big|_{\Gamma 1} \equiv 0, \bar{v}\big|_{\Gamma} \equiv 0, \bar{u}\big|_{\Gamma_1} = 0, \bar{v}\big|_{\Gamma_2} = 0, \\ \bar{\psi}(0,y) = \bar{\psi}(L,y) = \begin{cases} 0, y \in [0, H-\Delta], \\ \frac{1}{L}\left(y + \frac{2}{3}\Delta - H - \frac{(y-H)^3}{3\Delta^2}\right), y \in [H-\Delta, H], \\ \frac{2}{3}\frac{\Delta}{L} = const, y = H, \forall x \in [0,L]. \end{cases} \end{cases} \tag{22}$$

$$\bar{u}(0,y) = \bar{u}(L,y) = \frac{u(y)}{u_{\max}} = \begin{cases} 0, y \in [0, H-\Delta], \\ \left(1 - \frac{(y-H)^2}{\Delta^2}\right), y \in [H-\Delta, H]. \end{cases}$$

The remaining equations of problem (22) are the same as in problem (4). According to the general algorithm (step 6), it is necessary to compute the vorticity w at the boundary of the rectangle and then solve the vorticity equation (19) at the interior nodes of the cavity.

In the linear approximation, we assume that velocity, vorticity, and stream function at the boundary and the nearest interior nodes are linked by a single linear quadrature formula. The boundary values of the vorticity are approximated with fourth-order accuracy [10], since in [1] only first- and second-order formulas were given:

$$\psi_{xx}(0) = \frac{1}{h_1^2}\left(C_0\psi_0 + C_1\psi_1 + C_2\psi_2 + C_3\psi_3 + C_4\psi_4\right) + \frac{C_5\psi_x(0)}{h_1} = \frac{1}{h_1^2}\left(C_0\psi_0 + \sum_{i=1}^{4}\sum_{k=0}^{\infty} C_i \cdot \frac{(ih_1)^k \psi_0^{(k)}}{k!}\right) + \frac{C_5\psi_x(0)}{h_1} =$$

$$= \frac{\psi_0}{h_1^2}\left(C_0 + C_1 + C_2 + C_3 + C_4\right) + \frac{\psi_x(0)}{h_1}\left(C_1 + 2C_2 + 3C_3 + 4C_4 + C_5\right) + \psi_{xx}(0)\left(\frac{C_1}{2} + 2C_2 + \frac{9}{2}C_3 + 8C_4\right) +$$

$$+ h_1\psi_x^{(3)}(0)\left(\frac{C_1}{6} + \frac{8}{6}C_2 + \frac{27}{6}C_3 + \frac{64}{6}C_4\right) + h_1^2\psi_x^{(4)}(0)\left(\frac{C_1}{24} + \frac{16}{24}C_2 + \frac{81}{24}C_3 + \frac{256}{24}C_4\right) +$$

$$+ h_1^3\psi_x^{(5)}(0)\left(\frac{C_1}{120} + \frac{32}{120}C_2 + \frac{243}{120}C_3 + \frac{1024}{120}C_4\right) + O\left(h_1^4\right).$$

$$\Leftrightarrow \begin{cases} C_0 + C_1 + C_2 + C_3 + C_4 = 0 \\ C_1 + 2C_2 + 3C_3 + 4C_4 + C_5 = 0 \\ C_1 + 4C_2 + 9C_3 + 16C_4 = 2 \\ C_1 + 8C_2 + 27C_3 + 64C_4 = 0 \\ C_1 + 16C_2 + 81C_3 + 256C_4 = 0 \\ C_1 + 32C_2 + 243C_3 + 1024C_4 = 0 \end{cases} \Leftrightarrow C_0 = -\frac{415}{72}, C_1 = 8, C_2 = -3, C_3 = \frac{8}{9}, C_4 = -\frac{1}{8}, C_5 = -\frac{25}{6}.$$

Taking (22) into account, we obtain the general boundary condition for vorticity in the open cavity with fourth-order accuracy by differentiating (22) twice with respect to *y*:

$$w(x,y) = -\psi_{xx} - \psi_{yy} = \frac{1}{h_1^2}\left(\frac{415}{72}\psi_0 - 8\psi_1 + 3\psi_2 - \frac{8}{9}\psi_3 + \frac{1}{8}\psi_4\right) - \frac{25}{6}\frac{v(0,y)}{h_1} - \psi_{yy}, v = -\psi_x. \tag{23}$$

$$\overline{w}_{m,0} = \begin{cases} \frac{1}{h_1^2}\left(\frac{415}{72}\overline{\psi}_{m,0} - 8\overline{\psi}_{m,1} + 3\overline{\psi}_{m,2} - \frac{8}{9}\overline{\psi}_{m,3} + \frac{1}{8}\overline{\psi}_{m,4}\right) - \frac{25}{6}\frac{\overline{v}_{m,0}}{h_1} + 2\frac{(\overline{y_m} - H/L))}{(\Delta/L)^2}, m = \overline{n_3, n_2}, \\ \frac{1}{h_1^2}\left(\frac{415}{72}\overline{\psi}_{m,0} - 8\overline{\psi}_{m,1} + 3\overline{\psi}_{m,2} - \frac{8}{9}\overline{\psi}_{m,3} + \frac{1}{8}\overline{\psi}_{m,4}\right) - \frac{25}{6}\frac{\overline{v}_{m,0}}{h_1}, m = \overline{0, n_3}, left. \end{cases} \tag{24.1}$$

$$\overline{w}_{0,n} = \begin{cases} \frac{1}{h_2^2}\left(\frac{415}{72}\overline{\psi}_{0,n} - 8\overline{\psi}_{1,n} + 3\overline{\psi}_{2,n} - \frac{8}{9}\overline{\psi}_{3,n} + \frac{1}{8}\overline{\psi}_{4,n}\right) + \frac{25}{6}\frac{\overline{u}_{0,n}}{h_2}, n = \overline{0, n_1}, u = \psi_y, bottom, \\ \frac{1}{h_2^2}\left(\frac{415}{72}\overline{\psi}_{n_2,n} - 8\overline{\psi}_{n_2-1,n} + 3\overline{\psi}_{n_2-2,n} - \frac{8}{9}\overline{\psi}_{n_2-3,n} + \frac{1}{8}\overline{\psi}_{n_2-4,n}\right) - \frac{25}{6}\frac{\overline{u}_{n_2,n}}{h_2}, n = \overline{0, n_1}, top. \end{cases} \tag{24.2}$$

$$\overline{w}_{0,n} = \begin{cases} \frac{1}{h_2^2}\left(\frac{415}{72}\overline{\psi}_{0,n} - 8\overline{\psi}_{1,n} + 3\overline{\psi}_{2,n} - \frac{8}{9}\overline{\psi}_{3,n} + \frac{1}{8}\overline{\psi}_{4,n}\right) + \frac{25}{6}\frac{\overline{u}_{0,n}}{h_2}, n = \overline{0, n_1}, u = \psi_y, bottom, \\ \frac{1}{h_2^2}\left(\frac{415}{72}\overline{\psi}_{n_2,n} - 8\overline{\psi}_{n_2-1,n} + 3\overline{\psi}_{n_2-2,n} - \frac{8}{9}\overline{\psi}_{n_2-3,n} + \frac{1}{8}\overline{\psi}_{n_2-4,n}\right) - \frac{25}{6}\frac{\overline{u}_{n_2,n}}{h_2}, n = \overline{0, n_1}, top. \end{cases} \tag{24.3}$$

Unlike the closed-cavity case treated in [2], where derivatives of the vorticity function up to fifth order are computed explicitly, in problems (4) and (22) the application of formula (23) is appropriate. In fields with discontinuities of velocity the vorticity and its partial derivatives may attain large values. In deriving formula (23) derivatives of the stream function above second order were discarded. Table 1 gives a classification of blood vessels.

Table 1

Classification of blood vessels

Type	Diameter	Blood velocity	Reynolds number Re	Governing system
Capillaries	(5–10) μm	(0.5–1.0) mm/s	0.00075–0.00300	(21)
Arterioles	(10–100) μmm	(0.5–10.0) cm/s	0.015–3.000	(21),(4)
Arteries	(2–10) mm	(10–40) cm/s	60–1200	(4)
Aorta	(2–3) cm	0.5 m/s	3000	(4)

For definiteness, we solve problem (22) numerically when Re < 1 and problem (4) when Re > 1 ($h_1 = h_2 = 0{,}01$).

Experience shows that for a rapid solution in arterioles one should choose an inertial time interval $\frac{L}{u_{\max}}$, whereas to solve the hydrodynamic problem for an arteriole aneurysm it is appropriate to use system (4) analogously to the aneurysm-in-artery case.

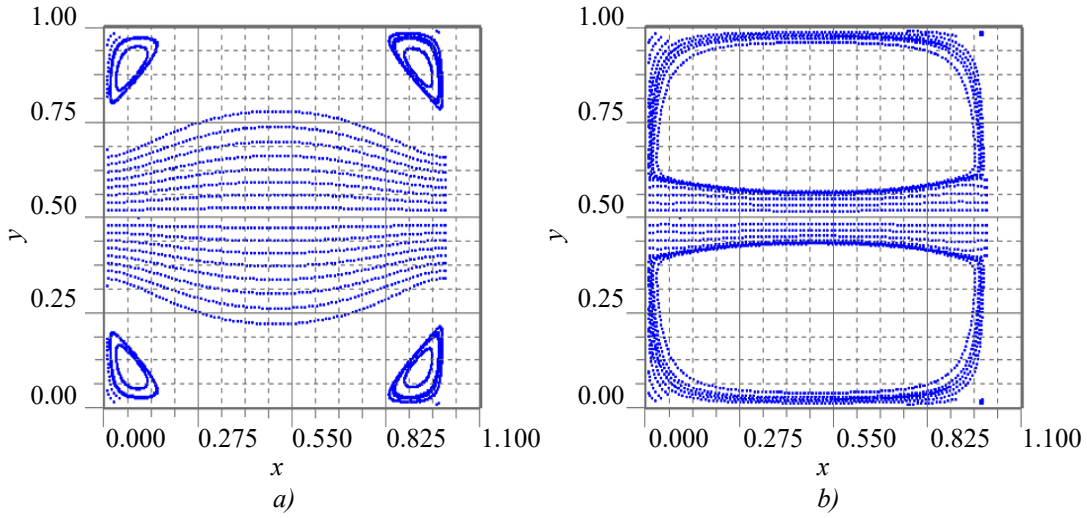

Fig. 3. Limiting streamline pattern in arterioles using formula (5.1):

a — Re = 0.75, $n_1 \times n_2 = 100 \times 50$, $\Delta / H = 0.5$; $L = 1$, $H = 50$ μ*m*, $u_{max} = 5$ *cm/s*, $\tau = \frac{6}{16} h_1^2$, $n = 400000$ steps, splitting multiplicity $m = 100$, $t = 0{,}512$ *s*; *b* — Re = 0.75, $n_1 \times n_2 = 100 \times 50$, $\Delta / H = 0.2$; $L = 1$, $H = 50$ μ*m*, $u_{max} = 5$ *cm/s*, $\tau = \frac{6}{16} h_1^2$, $n = 200000$ steps, splitting multiplicity $m = 100$, $t = 0.256$ *s*

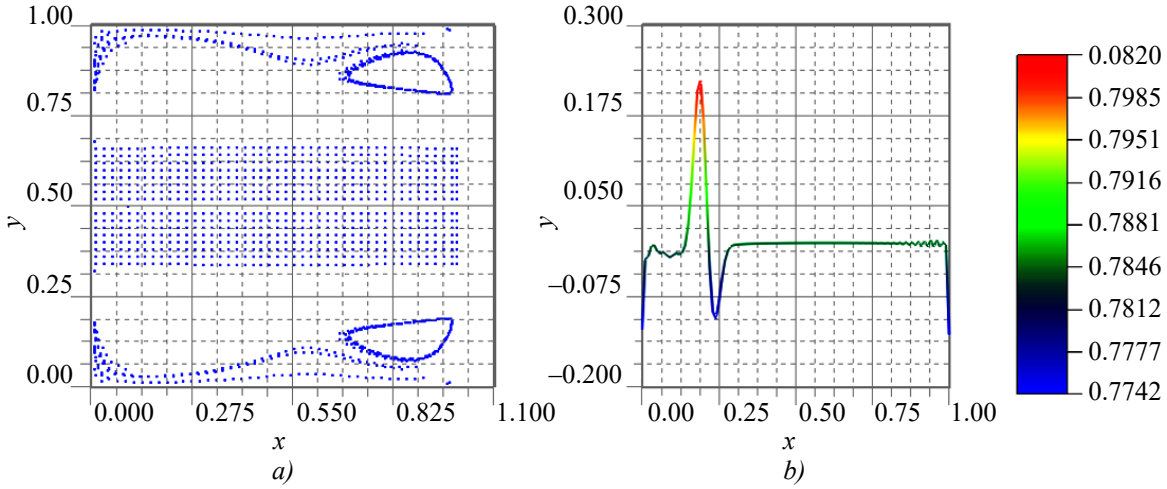

Fig. 4. Results of solving problem (4) with application of (5.1):

a — Re = 1500, $n_1 \times n_2 = 100 \times 50$, $\Delta / H = 0.6$; $L = 1$, $H = 1$ *cm*, $u_{max} = 50$ *cm/s*, streamline field in arteries after $n = 10000$ steps, splitting multiplicity $m = 200$; *b* — plot of the vorticity function in the symmetry plane

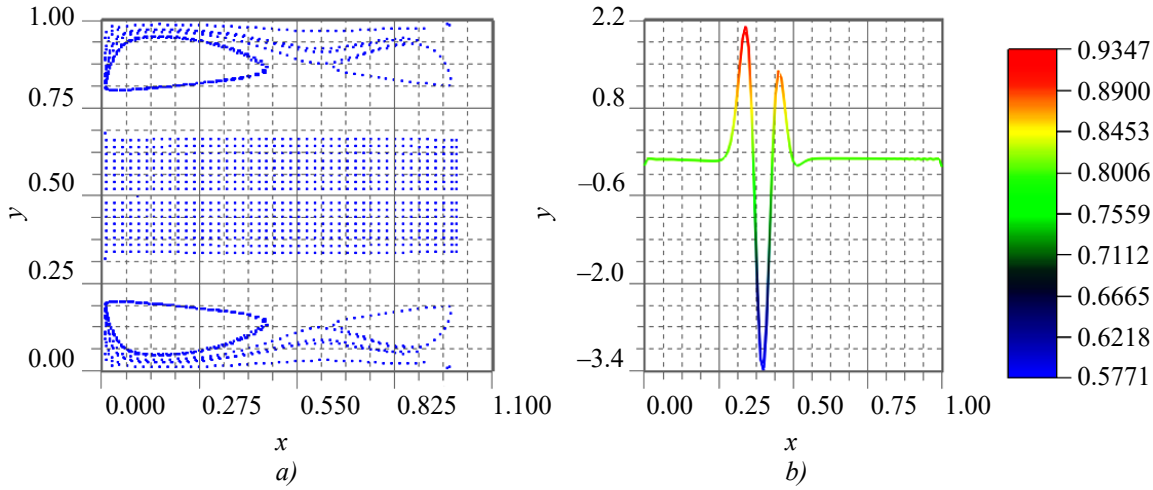

Fig. 5. Results of solving problem (4) with application of (5.1):

a — Re = 1500, $n_1 \times n_2 = 100 \times 50$, $\Delta / H = 0.6$; $L = 1$, $H = 1$ *cm*, $u_{max} = 50$ *cm/s*, streamline field in arteries after $n = 20000$ steps, splitting multiplicity $m = 200$; *b* — plot of the vorticity function in the symmetry plane

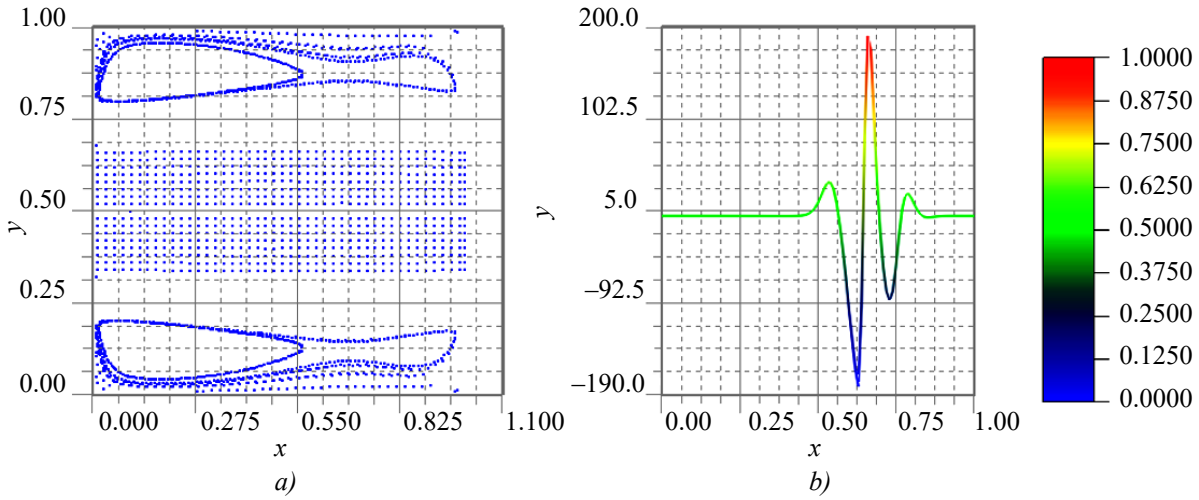

Fig. 6. Results of solving problem (4) with application of (5.1):
a — Re = 1500, $n_1 \times n_2 = 100 \times 50$, $\Delta / H = 0.6$; $L = 1$, $H = 1$ *cm*, $u_{max} = 50$ *cm/s* streamline field in arteries after $n = 34000$ steps, splitting multiplicity $m = 200$; *b* — plot of the vorticity function in the symmetry plane

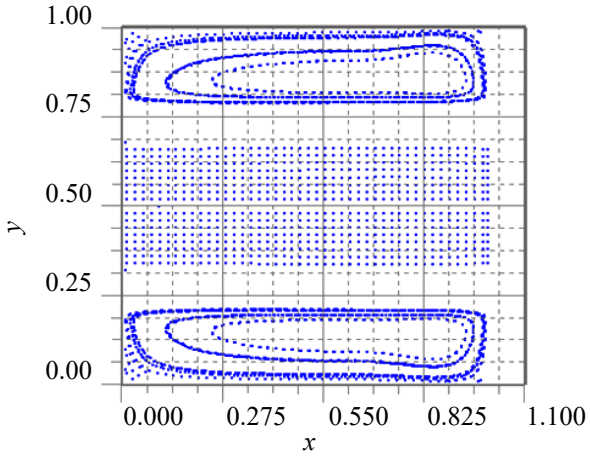

Fig. 7. Results of solving problem (4) with application of (5.2):
Re = 1500, $n_1 \times n_2 = 100 \times 50$, $\Delta / H = 0.6$; $L = 1$, $H = 1$ *cm*, $u_{max} = 50$ *cm*/s,
streamline field in the artery for $n = 2310000$ steps, splitting multiplicity $m = 200$

Discussion. Two numerical algorithms have been proposed for solving the two-dimensional problem in an open cavity ((5)–(21), (23), (24)) in the stream function–vorticity variables, modelling blood flow in an aneurysm under laminar (Re < 1 (22)) and turbulent (Re > 1, (4)) regimes.

In capillaries and arterioles (Fig. 3), the flow structure establishes within 0.002% of the period between pulsation waves (1 s). Therefore, the clot formation region is determined by the blood circulation region within the aneurysm.

The structure of circulation zones at low Reynolds numbers strongly depends on the ratio of the vessel diameter to the aneurysm diameter (Fig. 3). If the parameter , the circulation zone is located in the corners of the aneurysm (Fig. 3*a*). If the parameter , the circulation occupies the entire aneurysm (Fig. 3b), resulting in a narrowing of the channel diameter by 34%. This explains the phenomenon of "lumen constriction" during thrombus formation.

For high-speed flows (Re = 1500) in arteries and the aorta, the circulation region encompasses the entire aneurysm for any value of the parameter Δ / H ($\Delta / H = 0.6$) (Figs. 6*a* and 7).

Along the symmetry plane of the aneurysm, in the direction of blood flow, a sequence of alternating-sign vortices forms. In Fig. 4*b*, two vortices with signs *w* +, – appear. In Fig. 5*b*, three vortices with signs +, –, + are present. In Fig. 6*b*, five vortices form a sequence +, –, +, –, +. This chain of alternating-sign vortices resembles a Kármán vortex street in the wake of an obstacle.

The presence of vortices in the symmetry plane violates the assumption of solution symmetry. Therefore, it is necessary to allow for a nonzero normal velocity component in the symmetry plane and to include the entire aneurysm when solving

problem (4) for blood flow in the aorta. The formulations of problems (4) and (22) and their solution algorithms have been generalized for an open cavity, i. e., when cavity boundaries are intersected by fluid flows.

Conclusion. The initial-boundary value problems formulated in this study ((4), (22)) allow for a high-quality modelling of blood flow in aneurysms of capillaries, arterioles, and arteries at both low and high velocities, as well as blood flow in elements of medical devices.

References

1. Salih A. Streamfunction — Vorticity Formulation. *Department of Aerospace Engineering Indian Institute of Space Science and Technology.* 2013;10:1–10.

2. Volosova N.K., Volosov K.A., Volosova A.K., Karlov M.I., Pastukhov D.F., Pastukhov Yu.F. Comparison of solution of the hydrodynamic problem in a rectangular cavity methods of inhibition and acceleration of the initial speed field. *Computational Mathematics and Information Technologies*. 2025;9(2):22–33 (In Russ.) https://doi.org/10.23947/2587-8999-2025-9-2-22-33

3. Petrov A.G. High-precision numerical schemes for solving plane boundary value problems for a polyharmonic equation and their application to problems of hydrodynamics. *Applied Mathematics and Mechanics*. 2023;87(3):343–368 (In Russ.) https://doi.org/10.31857/S0032823523030128

4. Sukhinov A.I., Kolgunova O.V., Ghirmay M.Z., Nahom O.S. A two -dimensional hydrodynamic model of coastal systems, taking into account evaporation. *Computation Mathematics and Information Technologies*. 2023;7(4):9–21. https://doi.org/10.23947/2587-8999-2023-7-4-9-21

5. Ershova T.Ya. Boundary value problem for a third-order differential equation with a strong boundary layer. *Bulletin of Moscow University. Episode 15: Computational mathematics and cybernetics*. 2020;1:30–39 (In Russ.) https://doi.org/10.3103/S0278641920010057

6. Sitnikova M.A., Skulsky O.I. Flow of momentary anisotropic fluid in thin layers. *Bulletin of Perm University. Mathematics. Mechanics. Informatics.* 2015;28(1):56–62 (In Russ.)

7. Volosov K.A., Vdovina E.K., Pugina L.V. Modeling of “pulsatile” modes of blood coagulation dynamics. *Math modeling.* 2014;26(12):14–32 (In Russ.)

8. Sidoryakina V.V., Solomaha D.A. Symmetrized versions of the Seidel and upper relaxation methods for solving two-dimensional difference problems of elliptic. *Computational Mathematics and Information Technologies*. 2023;7(3):12–19. (In Russ.) https://doi.org/10.23947/2587-8999-2023-7-3-12-19

9. Volosova N.K., Volosov K.A., Volosova A.K., Karlov M.I., Pastuhov D.F., Pastuhov Yu.F. The *N*-fold distribution of the obvious variable scheme for the equalization of the vortex in the viscous incompatible fluid. *Bulletin of the Perm University. Mathematics. Mechanics. Informatics*. 2023;63(4):12–21 (In Russ.) https://doi.org/10.17072/1993-0550-2023-4-12-21

10. Bahvalov N.S., Zhidkov N.P., Kobelkov G.M. *Numerical methods: a textbook for students of physics and mathematics specialties of higher educational institutions Binom. lab*. Moscow: Knowledge; 2011. 636 p. (In Russ.)

About the Authors:

Natalya K. Volosova, Post-graduate Student of Bauman Moscow State Technical University (2nd Baumanskaya St. 5–1, Moscow, 105005, Russian Federation), ORCID, navalosova@yandex.ru

Konstantin A. Volosov, Doctor of Physical and Mathematical Sciences, Professor of the Department of Applied Mathematics of the Russian University of Transport (Obraztsova St. 9–9, Moscow, GSP-4, 127994, Russian Federation), ORCID, SPIN-code, konstantinvolosov@yandex.ru

Aleksandra K. Volosova, Candidate of Physical and Mathematical Sciences, Chief Analytical Department “Tramplin” LLC, Russian University of Transport (Obraztsova St. 9–9, Moscow, GSP-4, 127994, Russian Federation), ORCID, SPIN-code, alya01@yandex.ru

Mikhail I. Karlov, Candidate of Physical and Mathematical Sciences, Associate Professor of the Department of Mathematics, Moscow Institute of Physics and Technology (9, Institutsky Lane, GSP-4, Dolgoprudny, 141701, Russian Federation), SPIN-code, karlov.mipt@gmail.com

Dmitriy F. Pastukhov, Candidate of Physical and Mathematical Sciences, Associate Professor of Polotsk State University (Blokhin St. 29, Novopolotsk, 211440, Republic of Belarus), ORCID, SPIN-code, dmitrij.pastuhov@mail.ru

Yuriy F. Pastukhov, Candidate of Physical and Mathematical Sciences,Associate Professor of Polotsk State University (Blokhin St. 29, Novopolotsk, 211440, Republic of Belarus), ORCID, SPIN-code, pulsar1900@mail.ru

Contributions of the authors:

N.K. Volosova: setting the task; writing a draft of the manuscript; formulation of research ideas, goals and objectives.
K.A. Volosov: scientific guidance; methodology development.
A.K. Volosova: translation; study of the history of the task; literature.
M.I. Karlov: formal analysis.

D.F. Pastukhov: visualization; validation; software.
Yu.F. Pastukhov: testing of existing code components.

Conflict of Interest Statement: **the authors declare no conflict of interest.**

All authors have read and approved the final manuscript.

Об авторах:

Наталья Константиновна Волосова, аспирант Московского государственного технического университета им. Н.Э. Баумана (105005, Российская Федерация, г. Москва, ул. 2-я Бауманская, 5, стр. 1), ORCID, navalosova@yandex.ru

Константин Александрович Волосов, доктор физико-математических наук, профессор кафедры прикладной математики Российского университета транспорта (127994, ГСП-4, Российская Федерация, г. Москва, ул. Образцова, 9, стр. 9), ORCID, SPIN-код, konstantinvolosov@yandex.ru

Александра Константиновна Волосова, кандидат физико-математических наук, начальник аналитического отдела ООО «Трамплин» Российского университета транспорта (127994, ГСП-4, Российская Федерация, г. Москва, ул. Образцова, 9, стр. 9), ORCID, SPIN-код, alya01@yandex.ru

Михаил Иванович Карлов, кандидат физико-математических наук, доцент кафедры математики Московского физико-технического института (141701, ГСП-4, Российская Федерация, г. Долгопрудный, Институтский переулок, 9), SPIN-код, karlov.mipt@gmail.com

Дмитрий Феликсович Пастухов, кандидат физико-математических наук, доцент кафедры технологий программирования Полоцкого государственного университета (211440, Республика Беларусь, г. Новополоцк, ул. Блохина, 29), ORCID, SPIN-код, dmitrij.pastuhov@mail.ru

Юрий Феликсович Пастухов, кандидат физико-математических наук, доцент кафедры технологий программирования Полоцкого государственного университета (211440, Республика Беларусь, г. Новополоцк, ул. Блохина, 29), ORCID, SPIN-код, pulsar1900@mail.ru

Заявленный вклад авторов:

Н.К. Волосова: постановка задачи; написание черновика рукописи; формулировка идей исследования, целей и задач.
К.А. Волосов: научное руководство; разработка методологии.
А.К. Волосова: перевод; изучение истории задачи; поиск литературы.
М.И. Карлов: формальный анализ.
Д.Ф. Пастухов: визуализация; валидация; разработка программного обеспечения.
Ю.Ф. Пастухов: тестирование существующих компонентов кода.

Конфликт интересов: **авторы заявляют об отсутствии конфликта интересов.**

Все авторы прочитали и одобрили окончательный вариант рукописи.

Received / Поступила в редакцию 25.07.2025
Revised / Поступила после рецензирования 18.08.2025
Accepted / Принята к публикации 17.09.2025